A&A 488, L33–L36 (2008)
DOI: 10.1051/0004-6361:200810333

Astronomy & Astrophysics

Letter to the Editor

The properties of penumbral microjets inclination

J. Jurčák[1,2] and Y. Katsukawa[1]

[1] National Astronomical Observatory of Japan, 2-21-1 Osawa, Mitaka, Tokyo 181-8588, Japan
e-mail: jan.jurcak@nao.ac.jp
[2] Astronomical Institute of the Academy of Sciences, Fricova 298, 25165 Ondřejov, Czech Republic
e-mail: jurcak@asu.cas.cz

Received 6 June 2008 / Accepted 15 July 2008

ABSTRACT

Aims. We investigate the dependence of penumbral microjets inclination on the position within penumbra.
Methods. The high cadence observations taken on 10 November 2006 with the Hinode satellite through the Ca II H and G-band filters were analysed to determine the inclination of penumbral microjets. The results were then compared with the inclination of the magnetic field determined through the inversion of the spectropolarimetric observations of the same region.
Results. The penumbral microjet inclination is increasing towards the outer edge of the penumbra. The results suggest that the penumbral microjet follows the opening magnetic field lines of a vertical flux tube that creates the sunspot.

Key words. sunspots – Sun: chromosphere – Sun: photosphere – Sun: magnetic fields

1. Introduction

Katsukawa et al. (2007, hereafter Paper I) reported on the existence of small jet-like features that are observed at penumbral chromospheric layers. The authors used the term penumbral microjets (PJ) and this nomenclature is also used in this Letter. These new penumbral phenomena were found using the observations taken with the Hinode satellite through the broadband Ca II H filter.

As summarised in Paper I, the PJs are highly transient events with lifetimes up to two minutes and lengths of a few thousand kilometres. The width of PJs is around 400 km for the largest ones where the smallest events are at the resolution limit of the observations. It can be expected that there are even smaller undetected penumbral microjets.

As explained in Paper I, the three-dimensional configuration of the PJs can be estimated from the different visibilities of these events depending on the position on the solar disc. The intensity of microjets is comparable to the intensity of underlaying penumbral filaments, and the PJs can hardly be identified on observations taken close to the disc centre (if the running-difference or the high-pass filter are not applied). It implies that the azimuthal orientation of PJs is the same as for penumbral filaments, i.e., radial. In the case of observations taken farther from the disc centre, the microjets become visible due to the difference in their inclination compared to the inclination of penumbral filaments that are nearly horizontal. In Paper I the authors estimated the inclinations (angle between the local normal line and the microjet) to be mostly between 40° and 60°.

Although the observations with a cadence of four seconds can be achieved (with a limited field of view and only for a short time), the observations of penumbra with a 20 s cadence are currently the best available measurements that can be used to study the properties of PJs. Taking the lifetimes of PJs into account, the available high-cadence observations are not fast enough to study the photospheric counterparts of the PJs onsets because the original formation area can become dark in 20 s. As already pointed out in Paper I, there are some indications that the PJs are related to the penumbral bright grains observed in the photosphere. However, this topic is not discussed in this Letter and we concentrate on a detailed analysis of the penumbral microjets inclination and its dependence on the position within the penumbra. The results are then compared with the inclination of the photospheric magnetic field.

2. Observations and data reduction

We analysed the same data set as in Paper I. These measurements were taken on 10 November 2006, and they cover a part of the sunspot in AR10923, which was located at that time at heliocentric coordinates of 6° S and 50° E. Although there are some other observations of sunspots taken with a 30 s cadence far from the disc centre, they are either short in time or the penumbra is of small size so the statistical sample of detected PJs is too small for the purpose of our study.

The data were taken using the Solar Optical Telescope (SOT, Tsuneta et al. 2008) onboard Hinode satellite (Kosugi et al. 2007). The measurements are unaffected by atmospheric seeing, and the spatial resolution reaches the diffraction limit of the 50 cm telescope, i.e., 0.2″ (150 km) for the filtergram (FG) data and 0.32″ for spectropolarimetric (SP) data.

The analysed FG data were obtained through two broadband filters, the Ca II H (centred at 396.9 nm with bandwidth of 0.3 nm) and G-band filter (centred at 430.5 nm with bandwidth of 0.8 nm). The observations took place between 12:15 and 13:59 UT and are composed of 209 consecutive images. The data were calibrated with standard routines available under Hinode Solarsoft. The images in the sequence were aligned to compensate for the drift of the correlation tracker. The G-band and Ca II H images were carefully aligned. Figure 1a shows the first G-band image of the sequence with the estimated position of the umbral/penumbral and penumbral/quiet sun boundary.

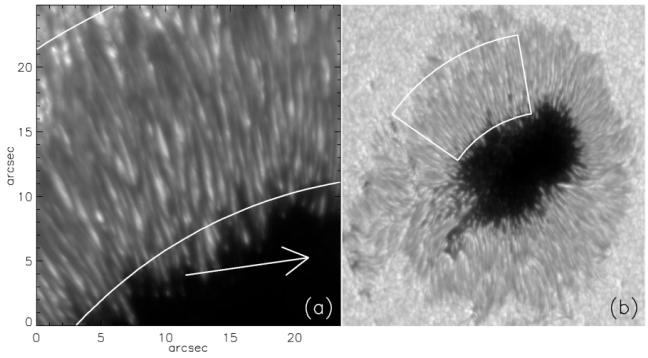

Fig. 1. The G-band image of the analysed area **a)**, where the lines mark the position of umbral/penumbral and penumbral/quiet sun boundary and the arrow points to the disc centre. The map of continuum intensity of the whole sunspot in AR10923 was reconstructed from the SP raster scan **b)**; see the text for details.

To determine the orientation of the magnetic field, we used the data observed by the Hinode SP. The measurements were taken in so-called normal mode; the width of the slit is equivalent to 0.16″ and comparable to the scanning step; the exposure time for one slit position is 4.8 s and results in a noise level of 10^{-3} I_c. More detailed information about this SP observation mode and the reduction of SP data can be found in Jurčák et al. (2007). The necessary calibration of wavelengths and the normalisation of the observed Stokes profiles to the continuum intensity of the Harvard Smithsonian reference atmosphere is also described there. Figure 1b shows part of the continuum intensity map reconstructed from the SP raster scan of AR10923. The framed part of the penumbra roughly corresponds to the area observed with FG. The raster scan of the marked region was taken between 16:25 and 16:40 UT, approximately 3 h later than FG measurements.

3. Estimation of position and inclination

The alignment between FG and SP data cannot be done precisely since the penumbra was slowly growing in the meantime between the observations. The alignment of the inner and outer penumbral boundaries in FG and SP data is sufficient for the purpose of our study since we do not take the azimuthal positions into account and the possible inaccuracies in the estimated radial positions would not affect the results.

The penumbral boundaries are approximately fitted by concentric arcs as shown in Fig. 1a for FG data and in Fig. 1b for SP data. The position of PJ in the penumbra is given by the radius of an arc that crosses the detected onset of the microjet as shown in Fig. 2b.

3.1. Penumbral microjet inclination

To compute the inclination angle of the PJs, we first manually determined the orientation of the microjet either directly from Ca II H data or using running-difference images. Figures 2a and c show examples of four PJs. The orientations of penumbral filaments are determined from G-band images, Fig. 2b. Knowing the heliocentric angle and the orientation of the symmetry line (that connects the disc centre and the microjet onset position) for each analysed PJ, we can use the following equation (Müller et al. 2002)

$$\phi = \arctan\left(\frac{\sin\gamma' \sin\phi'}{\cos\gamma' \sin\theta + \sin\gamma' \cos\phi' \cos\theta}\right), \quad (1)$$

where θ is the heliocentric angle, ϕ the azimuth angle in line-of-sight (LOS) frame, and ϕ' and γ' represent the azimuth and inclination in the local reference frame (LRF) that is defined by the local normal line (z axis) and the orientation of the symmetry line (x axis).

Our final goal is to determine the LRF inclination of the PJ ($\gamma'_{\rm PJ}$). From the observations we know the heliocentric angle (θ, around 51°) and the LOS azimuths of microjet ($\phi_{\rm PJ}$, the angle between the symmetry line and the PJ) and filament ($\phi_{\rm F}$, the angle between the symmetry line and the penumbral filament). As shown in Paper I, we can suppose that the azimuthal orientation of the PJs is the same as for the penumbral filaments in the LRF ($\phi'_{\rm PJ} = \phi'_{\rm F}$).

To determine the $\phi'_{\rm F}$ and thus also $\phi'_{\rm PJ}$, we need to estimate the elevation angle of the penumbral filaments. They are not exactly horizontal since the Wilson depression must be compensated for in the penumbra. The exact value of the filaments elevation angle is unknown. We estimate it to be 5° with respect to the local horizontal line. This value corresponds to the difference found between the filament orientation and the magnetic field azimuth (Lites & Skumanich 1990; Westendorp Plaza et al. 2001) that can be caused by the elevation of penumbral filaments, although there are other possible scenarios for this difference.

The assumption of a 5° elevation angle gives us the inclination of penumbral filament in LRF ($\gamma'_{\rm F}$) as 85°. Thus, we know θ, $\gamma'_{\rm F}$, and $\phi_{\rm F}$, and Eq. (1) can be used to derive the LRF azimuth value $\phi'_{\rm F}$ that also represents the LRF azimuth of the PJ ($\phi'_{\rm PJ}$). Knowing θ, $\phi'_{\rm PJ}$, and $\phi_{\rm PJ}$, Eq. (1) can be used again to derive the value of $\gamma'_{\rm PJ}$ that represents the inclination of the microjet in the LRF. In Fig. 2c the derived values are shown for each of the four depicted jets.

We estimate the error of individually determined inclination values to be up to 10°. This uncertainty comes from the manual estimation of the PJ and filament orientation and becomes even greater in the outer penumbra where the filament direction could be difficult to estimate from G-band images, and the microjets are less apparent in Ca II H data due to the increased intensity of underlying material. Another source of uncertainty is the incorrect estimation of the onset of PJs. This might result in selecting the wrong filament in the G-band image.

The unknown value of the penumbral filament elevation, and its possible dependence on position within the penumbra causes a further increase in the error. We estimate this error to be in the order of a few degrees. No strong dependence of this value on the position within the penumbra is expected, as the absolute values of the elevation angle are expected to be small. Therefore, the change in PJs inclinations across the penumbra is not significantly influenced.

3.2. Magnetic field inclination

The Stokes profiles observed at pixels in the marked area in Fig. 1b are inverted using the SIR code (Stokes Inversion based on Response functions; Ruiz Cobo & del Toro Iniesta 1992). Taking the high spatial resolution of the Hinode SP measurements into account, we use only a one-component atmospheric model. However, given the observed asymmetries of Stokes profiles, we allow for the changes in plasma parameters with height in the atmosphere.

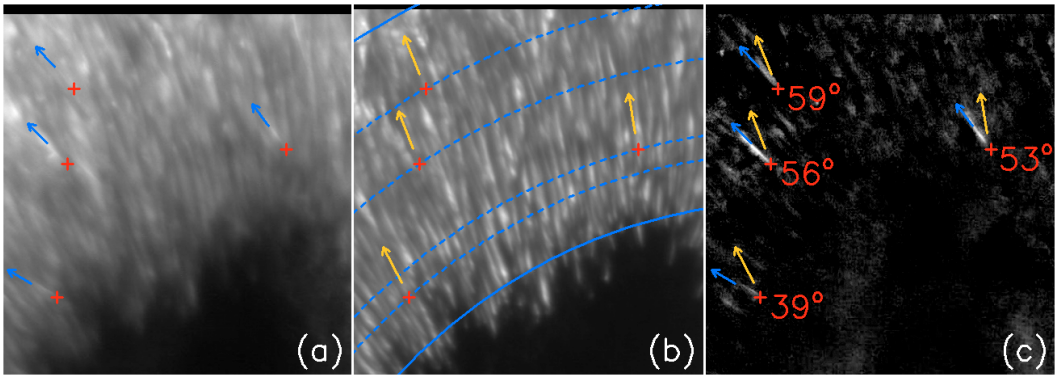

Fig. 2. The Ca II H **a)**, G-band **b)**, and Ca II H running-difference **c)** images of the analysed area. The red crosses mark the identified onsets of PJs, the blue arrows indicate their orientation, and the orange arrows point in the direction of penumbral filaments. The blue lines show the inner and outer edges of the penumbra (solid) and the position of PJs (dashed). The resulting values of LRF inclinations are shown in the **c)** image.

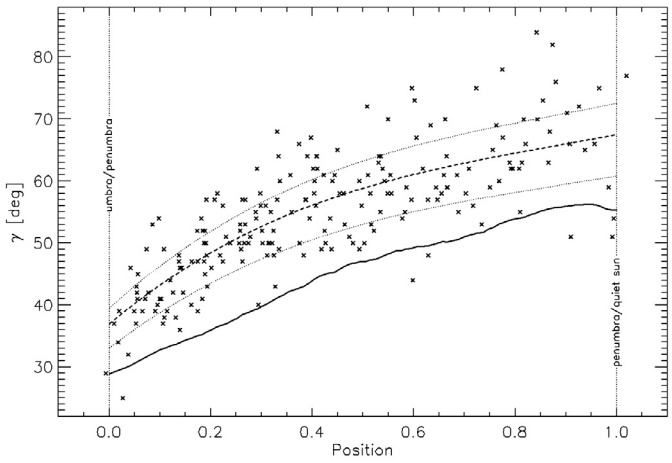

Fig. 3. The plot shows the dependence of microjet inclination on the position within the penumbra. The 209 detected PJs are represented by × symbols. The dashed line is a third-order polynomial fit of the observed distribution of microjet inclination through the penumbra, where the dotted lines are the alternatives obtained for different values of penumbral filament elevation; 0° and 8° for the lower and upper dotted line, respectively. The solid line shows the inclination of magnetic field at high photospheric layers. The position of umbra/penumbra and penumbra/quiet sun boundary are taken as 0 and 1, respectively.

The derived values of magnetic field inclination and azimuth are evaluated with respect to the LOS. After the transformation to the LRF, we determine the single value of magnetic field inclination at each pixel. As the PJs take place in the chromosphere, we want to determine the magnetic field inclination at the highest possible layers of photosphere. According to Cabrera Solana et al. (2005), the observed pair of iron lines is the most sensitive to plasma parameters in the range of optical depths between $\log(\tau) = -1$ and -2. As the height in the atmosphere increases with decreasing $\log(\tau)$, we use the average value of inclination from the range of $\log(\tau) = \langle -1.5, -2 \rangle$. Azimuthal averages over pixels with the same position in the penumbra are computed to obtain a curve that shows the magnetic field inclination as a function of the radial distance in the penumbra.

The obtained curve (solid line in Fig. 3) is comparable in absolute values to the inclinations of the so-called background component of the penumbral atmosphere obtained from two-component inversions (Bellot Rubio et al. 2004; Borrero et al. 2006). The concept of two-components comes from the uncombed model of penumbral atmosphere (Solanki & Montavon 1993; Martínez Pillet 2000), where the background component has a stronger and more vertical magnetic field compared to the second component and represents the properties of a vertical flux tube that creates the sunspot. The obtained similarity between the inclination values at higher photospheric layers and the background component inclination confirms that the horizontal fields presented in the penumbra are restricted to the lower part of the line-forming region (Bellot Rubio et al. 2006; Jurčák et al. 2007). Our findings can be also understood in terms of the cusp model introduced by Scharmer & Spruit (2006) where the horizontal fields are restricted to the lowest photosphere, and the magnetic field at the higher layers is also that of the vertical flux tube.

4. Comparison of inclination

In Fig. 3, the inclination of 209 individual PJs identified at various positions within the penumbra (× symbols) are shown and the mean behaviour of PJs inclination (dashed line) is compared with the radial variation of the magnetic field inclination (solid line). It appears that there is an almost constant difference between the mean inclination of chromospheric PJs and the magnetic field in the photosphere, the former one being more horizontal by about 10°, that is, if we take the 5° elevation angle of penumbral filaments into account. Even if we suppose that the filaments are exactly horizontal (lower dotted line), the PJs are still more inclined than the magnetic field in the photosphere.

If we assume that these values of magnetic field inclination describe the orientation of the field lines of an vertical flux tube that creates the sunspot, then there is an apparent explanation for the more horizontal direction of PJs. Such a vertical flux tube has to be opening with height due to the pressure balance. If we follow one specific magnetic field line then this becomes more horizontal with height in the atmosphere. This can explain the relation and also the observed difference between the chromospheric microjets and the photospheric magnetic field. A microjet following an opening magnetic field line would appear more horizontal than this same field line at photospheric layers.

These assumptions also imply that the PJs would become more horizontal with height; i.e., the observed microjets should not be straight but instead bend towards the horizontal direction. There are only a few observed cases of PJs in the analysed data set that appear to be curved. We suppose that the rarity of curved PJs is mainly caused by the shortness of these events and by the projection effect to the LOS frame.

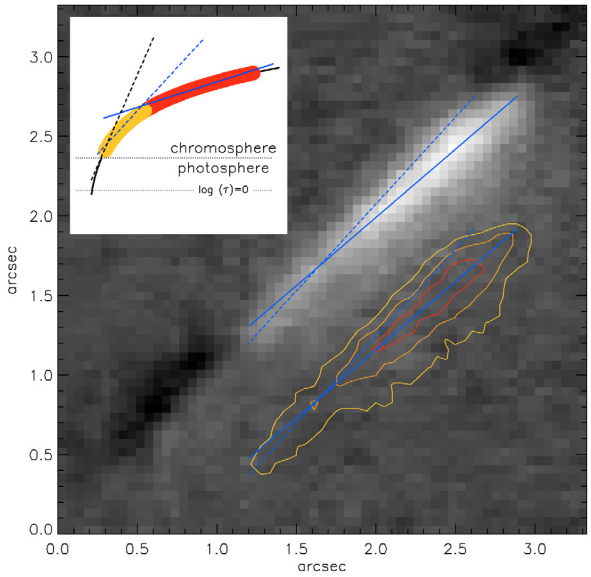

Fig. 4. The magnified running-difference image of one of the microjet that is slightly curved. The solid blue line is the linear fit of the brightest area of the microjet and the dashed blue line represent the initial orientation of the microjet. The intensity contours, drawn at an offset of –0.8″ along the *y*-axis are shown to emphasise the curvature of the PJ. A sketch of a penumbral microjet is shown in the upper left corner. The dashed and solid blue lines represent the orientation in the initial and later phase, respectively. The sketched PJ follows the opening field line marked by the solid black line and the dashed black line shows its inclination at higher photospheric layers.

Figure 4 shows the running-difference image of a microjet (bright area, detected onset is at lower left part of the image) that appears to be bending towards the horizontal line with height in the atmosphere. A simplified sketch of a microjet is plotted in the upper left corner of Fig. 4. There is a small change of PJ orientation between the faint part (initial phase, fitted by the dashed blue line) and the bright part (later phase, fitted by the solid blue line). In the case of the observed PJ, the angle between these lines is 7° in the LOS frame and corresponds to the difference of 9° in the LRF. This value is comparable to the average difference between the dashed and solid lines in Fig. 3; i.e., the initial inclination of this microjet is close to the magnetic field inclination at higher photospheric layers. From the simplified sketch it is also apparent, that the sooner the PJ is identified, the closer its inclination to the magnetic field inclination obtained at higher photospheric layers will be.

The results shown in Fig. 3 also imply that the field is becoming more horizontal with height along the local normal line anywhere in the penumbra. This does not agree with a simple conception of an opening flux tube that would result in approximately constant inclination values along the local normal line. Constant inclination with height was also found by Orozco Suarez et al. (2005), who used the inversion of spectral lines to determine the magnetic field orientation in photosphere and chromosphere. However, the authors assume that the magnetic field inclination is constant with height in the photosphere. Thus, the obtained photospheric inclinations might by influenced by the horizontal component of the magnetic field and are indeed higher than those obtained in this analysis or from the two-component inversions. The magnetic field inclinations at the chromospheric layers found by Orozco Suarez et al. (2005) are comparable to the PJ inclinations reported in this Letter.

5. Conclusions

We identified 209 penumbral microjets in almost two-hour long observations of the penumbra in AR10923 using the Ca II H images taken with 30 s cadence. In combination with simultaneous G-band observations, the inclinations of these microjets (angle between the PJ and local normal line) are determined along with their approximate position in the penumbra. The results show a clear increase in the PJ inclination toward the outer penumbral edge. We find on average inclinations around 35° at the umbra/penumbra boundary and 70° at the penumbra/quiet sun boundary.

The found radial variation in the PJ inclination resembles the change in magnetic field inclination at higher photospheric layers across the penumbra. We find the difference of 10° between the inclinations of magnetic field lines and penumbral microjets, with the former more vertical. This difference can be explained easily if we suppose that the PJs follow the magnetic field lines that are opening with height. There are a few observed PJs that show the change in inclination with height in the atmosphere and support this hypothesis.

The observed difference also implies that on average we detect the PJs at higher atmospheric layers and only rarely at the initial stage when the PJs inclination angles should be close to (or same as) the magnetic field inclination at higher photospheric layers. The scatter of individually determined values of PJs inclination in Fig. 3 can be influenced by the different time spans between the onset and the determination of the PJs inclination.

Although our results cannot clarify the mechanism responsible for the formation of the PJs, they imply that the PJs are guided by magnetic field lines that are fanning out with height. Higher cadence observations of Ca II H and G-band filtergrams and simultaneous SP measurements are needed to study this problem in detail.

Acknowledgements. We thank Luis Bellot Rubio and Rolf Schlichenmaier for helpful suggestions and comments. This work was enabled thanks to the funding provided by the Japan Society for the Promotion of Science. Financial support from GA AS CR IAA30030808 is gratefully acknowledged. Hinode is a Japanese mission developed and launched by ISAS/JAXA, with NAOJ as domestic partner and NASA and STFC (UK) as international partners. It is operated by these agencies in cooperation with ESA and NSC (Norway). The computations were partly carried out at the NAOJ Hinode Science Center, which is supported by the Grant-in-Aid for Creative Scientic Research The Basic Study of Space Weather Prediction from MEXT, Japan (Head Investigator: K. Shibata), generous donations from Sun Microsystems, and NAOJ internal funding.

References

Bellot Rubio, L. R., Balthasar, H., & Collados, M. 2004, A&A, 427, 319
Bellot Rubio, L. R., Schlichenmaier, R., & Tritschler, A. 2006, A&A, 453, 1117
Borrero, J. M., Solanki, S. K., Lagg, A., Socas-Navarro, H., & Lites, B. 2006, A&A, 450, 383
Cabrera Solana, D., Bellot Rubio, L. R., & del Toro Iniesta, J. C. 2005, A&A, 439, 687
Jurčák, J., Bellot Rubio, L., Ichimoto, K., et al. 2007, PASJ, 59, 601
Katsukawa, Y., Berger, T. E., Ichimoto, K., et al. 2007, Science, 318, 1594
Kosugi, T., Matsuzaki, K., Sakao, T., et al. 2007, Sol. Phys., 243, 3
Lites, B. W., & Skumanich, A. 1990, ApJ, 348, 747
Martínez Pillet, V. 2000, A&A, 361, 734
Müller, D. A. N., Schlichenmaier, R., Steiner, O., & Stix, M. 2002, A&A, 393, 305
Orozco Suarez, D., Lagg, A., & Solanki, S. K. 2005, in Chromospheric and Coronal Magnetic Fields, ed. D. E. Innes, A. Lagg, & S. A. Solanki, ESA Spec. Publ., 596
Ruiz Cobo, B., & del Toro Iniesta, J. C. 1992, ApJ, 398, 375
Scharmer, G. B., & Spruit, H. C. 2006, A&A, 460, 605
Solanki, S. K., & Montavon, C. A. P. 1993, A&A, 275, 283
Tsuneta, S., Ichimoto, K., Katsukawa, Y., et al. 2008, Sol. Phys., 249, 167
Westendorp Plaza, C., del Toro Iniesta, J. C., Ruiz Cobo, B., et al. 2001, ApJ, 547, 1130